JOURNAL OF Applied Polymer SCIENCE

Dielectric and Electrical Properties of an Organic Device Containing Benzotriazole and Fluorene Bearing Copolymer

Dilber Esra Yildiz,[1] Dogukan Hazar Apaydın,[2] Levent Toppare,[3,4,5] Ali Cirpan[2,3,5,6]

[1]Department of Physics, Faculty of Arts and Sciences, Hitit University, 19030 Çorum, Turkey
[2]Department of Polymer Science and Technology, Middle East Technical University, 06800 Ankara, Turkey
[3]Department of Chemistry, Middle East Technical University, 06800 Ankara, Turkey
[4]Department of Biotechnology, Middle East Technical University, 06800 Ankara, Turkey
[5]The Center for Solar Energy Research and Applications (GUNAM), Middle East Technical University, 06800 Ankara, Turkey
[6]Department of Micro and Nanotechnology, Middle East Technical University, 06800 Ankara, Turkey
Correspondence to: D. E. Yildiz (E-mail: desrayildiz@hitit.edu.tr)

ABSTRACT: Dielectric and electrical properties of a benzotriazole and fluorene copolymer were investigated using current-voltage (*I–V*), capacitance-voltage (*C–V*), and conductance–voltage (*G/w–V*) measurements at room temperature. The electrical parameters, barrier height (φ_{Bo}), and ideality factor (*n*) obtained from the forward bias *LnI-V* plot were found as 0.453 eV and 2.08, respectively. The R_s values were found as 2.20, 2.12, 1.90 Ω using *dV/dLnI* versus *I*, *H(I)* versus *I* and *F(V)-V* plots, respectively. The dielectric constant (ε'), the dielectric loss (ε''), and the ac electrical conductivity (σ_{ac}) are a strong function of voltage and frequency. Decrease in ε' and ε'' values with increasing frequency was observed. On the other hand, the increase of σ_{ac} with increasing frequency was observed .Experimental results show that the conjugated copolymer plays an important role in the values of barrier height, ideality factor, series resistance, and dielectric parameters. © 2012 Wiley Periodicals, Inc. J. Appl. Polym. Sci. 000: 000–000, 2012

KEYWORDS: copolymers; dielectric properties; properties and characterization

Received 25 May 2012; accepted 6 July 2012; published online
DOI: 10.1002/app.38315

INTRODUCTION

Conjugated copolymers are lighter, more flexible, and less expensive than inorganic conductors. This makes them a desirable alternative in many electronic and optoelectronic device applications.[1–4] It also creates the possibility of new solid-state electronic device applications that would be impossible using copper or silicon. There are a number of conjugated copolymers which can be used for the fabrication of electronic devices due to their unique electrical and optical properties. Among them, fluorene- and benzotriazole-based conjugated polymers have been intensely studied.[5–8] The use of fluorene and benzotriazole units revealed some promising features for photovoltaic applications and they attracted the attention of many scientists.[5–10]

Such devices are similar to metal/insulator/semiconductor (MIS) type Shottky barrier diodes. The performance of these devices is affected by the formation of interfacial copolymer layer and interface states (N_{ss}) at metal/copolymer interface and the formation of barrier height at MIS interface. Organic electronics not only includes organic semiconductors but also organic dielectrics. Therefore, it is important to study the electrical and dielectric properties of benzotriazole- and fluorene-based organic devices. The bias voltage dependence of *I–V* proved to be a powerful tool for studying electrical properties.[11–13] In addition, frequency dependence of *C* and *G/w* proved to be a powerful tool for studying the dielectric properties and can give detailed information on ε', ε'', and σ_{ac} of devices.[14–16]

In our previous study,[17] photovoltaic properties of poly((9,9-dioctylfluorene)-2,7-diyl-(4,7-bis(thien-2-yl) 2-dodecyl-benzo [1,2,3]triazole)) has been studied. In this study, we investigated the electrical (n,φ_B, R_s) and dielectric (ε', ε'', and tan δ) properties of benzotriazole- and fluorene-based organic devices at room temperature. The R_s was obtained using Norde and Cheung's methods. In addition, the frequency and voltage dependence of dielectric properties was obtained from the *C–V* and *G/w-V* measurements.

EXPERIMENTAL

The organic device was fabricated as ITO/PEDOT : PSS/Copolymer/Au configuration (Figure 1). Indium tin oxide (ITO)-coated glass substrates were etched and cleaned by ultrasonic

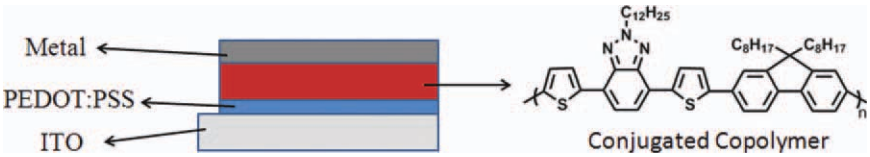

Figure 1. The schematic diagram of ITO/PEDOT : PSS/Copolymer/Au device and the molecular structure of the copolymer. [Color figure can be viewed in the online issue, which is available at wileyonlinelibrary.com.]

treatments in water, detergent, acetone, and isopropanol and later also treated in a Harrick Plasma Cleaner for 5 min. Then, a thin layer of PEDOT : PSS was spin coated on ITO substrate at 5000 rpm and baked at 130°C for 10 min on a hotplate. A thin layer of poly((9,9-dioctylfluorene)-2,7-diyl-(4,7-bis(thien-2-yl) 2-dodecyl-benzo[1,2,3] triazole)) was prepared by spin coating from chlorobenzene solution at 1200 rpm. The thickness of copolymer was found to be 80 nm from AFM studies. The cathode was thermally evaporated as a 100 nm Au layer at a pressure of 2×10^{-6} mbar through a shadow mask. Devices were fabricated with an active area of 0.065 cm^2. The current– voltage characteristic measurements were carried out in MBraun glovebox (moisture <0.1 ppm; oxygen <0.1 ppm) under dark. The *C–V* and *G/w-V* characteristics of ITO/PEDOT : PSS/Copolymer/Au were carried out with a Keithley 4200 semiconductor analyzer in the frequency range of 10 kHz to 1 MHz at room temperature.

RESULTS AND DISCUSSION

Electrical Properties

The thermionic emission (TE) theory can be used to find electrical properties of the MS, MOS, and MIS structures. According to the pure TE theory, the current of a Schottky device or MIS-type devices with a series resistance can be expressed as[18,19]

$$I = I_0 \left[\exp\left(\frac{qV}{kT}\right) - 1\right] \tag{1}$$

where I_0 is saturation current and can be written as[20]

$$I_0 = AA^* T^2 \exp\left(-\frac{q\varphi_{Bo}}{kT}\right) \tag{2}$$

where q is the electronic charge, V is the applied voltage, k is the Boltzmann constant, T is the absolute temperature in K, n is the dimensionless ideality factor, R_s is the series resistance of structure, A is the effective area of the rectifier contact, A^* is the effective Richardson constant usually taken as 120 $A/cm^{-2}K^{-2}$ for free electron[21,22] and φ_{Bo} is the zero bias barrier height. When ITO/PEDOT : PSS/copolymer/Au device with R_s in considered, it assumed that the net current of the diode is due to TE theory and it can be expressed as $V \geq 3kT/q$

$$I = I_0 \left[\exp\left(\frac{q(V - IR_s)}{nkT}\right) - 1\right] \tag{3}$$

where (V-IR_s) is equal to the voltage drop across the diode (V_d). The reverse saturation current (I_0) was obtained by extrapolating the linear intermediate voltage region of the curve to zero-applied bias voltage.

$$\varphi_{Bo} = \frac{kT}{q} \ln\left(\frac{AA^* T^2}{I_0}\right) \tag{4}$$

$$n = \frac{q}{kT}\left(\frac{d(V - IR_s)}{d \ln I}\right) \tag{5}$$

Figure 2 shows the *I–V* characteristics of the devices at room temperature. The forward bias *I–V* exhibited a linear behavior at low bias voltage. However, it deviated from linearity at forward bias due to R_s effect and interfacial copolymer layer. The value of φ_{Bo} was calculated as 0.453 eV. The n for the device was obtained from the slope of the *I–V* curve (eq. 5) as 2.08. This value is greater than unity revealing a deviation from an ideal diode. This may be due to presence of an inhomogeneous organic layer.[23,24]

The value of R_s for MS, MIS devices is a parameter causing serious errors in calculating some electrical characteristics. Several methods were suggested in literature[25–27] for the determination

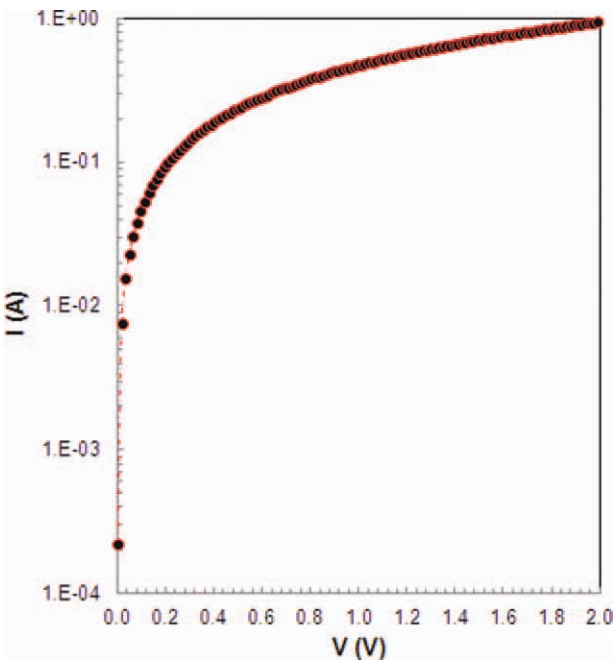

Figure 2. Forward and reverse bias semilogarithmic *I–V* characteristics of organic device. [Color figure can be viewed in the online issue, which is available at wileyonlinelibrary.com.]

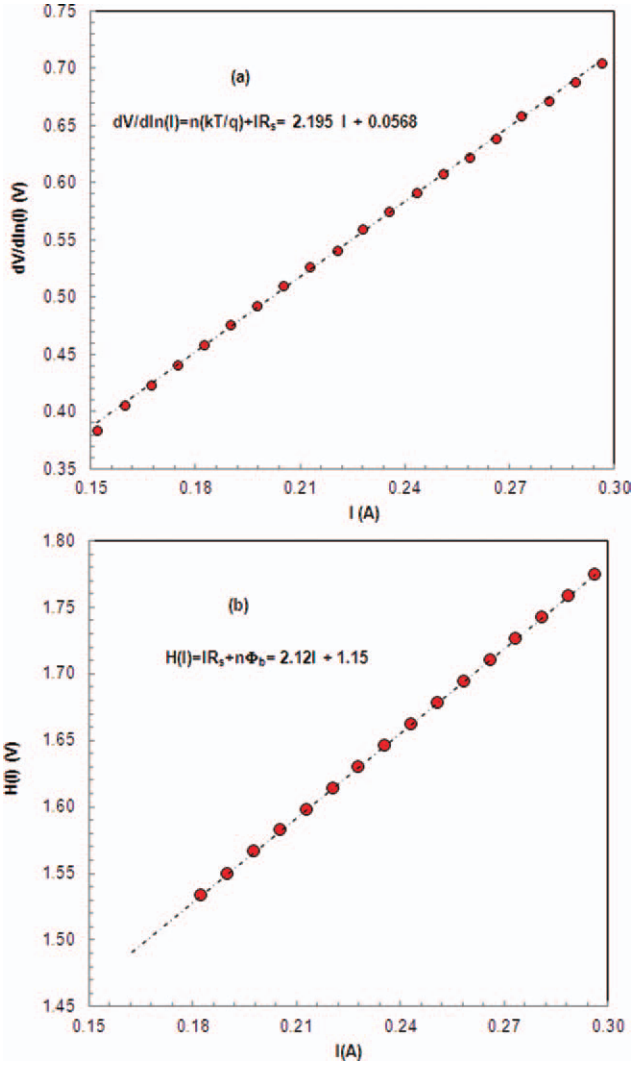

Figure 3. The experimental (a) *dV/dLnI* versus *I* plot (b) *H(I)* versus *I* plot of organic device. [Color figure can be viewed in the online issue, which is available at wileyonlinelibrary.com.]

of R_s. Cheung's and Norde methods are the frequently used ones for the determination of R_s.[28] The *n*, R_s, and φ_B were calculated using the Cheung's method for ITO/PEDOT : PSS/copolymer/Au devices. Cheung's function is defined as[28,29]

$$\frac{dV}{dLn(I)} = IR_s + \left(\frac{nkT}{q}\right) \tag{6a}$$

$$H(I) = V - \frac{nkT}{q} In\left(\frac{I_0}{AA * T^2}\right) = IR_s + n\varphi_B \tag{6b}$$

Experimental *dV/dLnI* versus *I* and *H(I)* vs *I* plots at room temperature for devices are shown in Figure 3(a,b). The slope of *dV/dLnI* versus *I* plot gives R_s and nkT/q as the intercept. The values of *n* and R_s were obtained as 2.195 and 2.20 Ω, respectively. The φ_B and R_s values were determined from the *H(I)-I* plot as 0.523 eV and 2.12 Ω. The poly((9,9-dioctylfluorene)-2,7-diyl-(4,7-bis(thien-2-yl)2-dodecyl-benzo[1,2,3]triazole)) has a low series resistance. On the other hand, copolymer morphology, bulk resistance, and space charge limited effects can cause a high ideality factor. In addition, the device electrical parameter can be also determined from the modified Norde function as:[25,27]

$$F(V) = \frac{V}{\gamma} - \frac{kT}{q}\left(\frac{I(V)}{AA^* T^2}\right) \tag{7a}$$

where γ is the first integer greater than n and $I(V)$ is the current for any bias voltage (V_i). The barrier height of the device can be obtained by using eq. (7b).[27]

$$\varphi_B = F(V_0) + \frac{V_0}{\gamma} - \frac{kT}{q} \tag{7b}$$

where $F(V_0)$ is the minimum $F(V)$ value of F versus V graph and V_0 is the corresponding. Figure 4 shows the $F(V)$-V graph of the structure. Thus, values of R_s can be calculated by Norde's method through the relation,[27]

$$R_s = \frac{kT(\gamma - n)}{qI} \tag{7c}$$

Using eqs. (8) and (9) the φ_B and R_s values were determined as 0.433 eV and 1.90 Ω respectively. It is clear that the values of R_s obtained from Cheung and Norde methods are in good agreement with the experimental R_s value.

The *C–V* and *G/w* plots in the frequency range of 10 kHz to1 MHz for the ITO/PEDOT : PSS/copolymer/Au device are shown in Figure 5(a,b). The values of *C* reveal a peak for each frequency and decrease with increasing frequency. The values of *G/w* show a U behavior for each frequency and decrease with increasing frequency. The existence of the maximum value of the peak in the *C–V* plot of MS and MIS structures has been explained by molecular restructuring and reordering of the interface states and series resistance.[28,29]

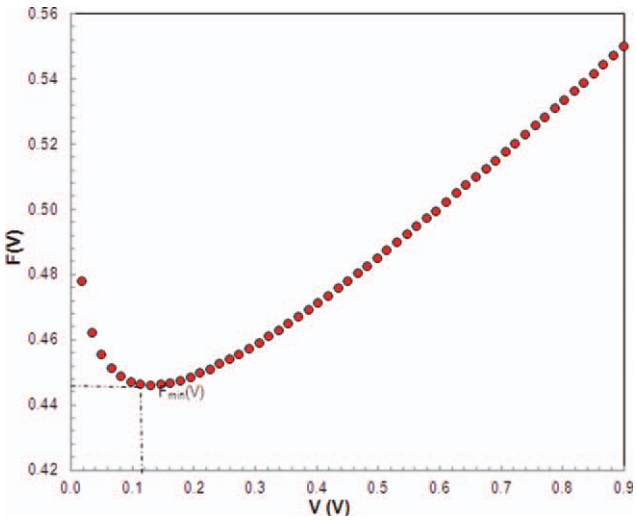

Figure 4. The experimental $F(V)$-V graph of organic device. [Color figure can be viewed in the online issue, which is available at wileyonlinelibrary.com.]

Applied Polymer SCIENCE

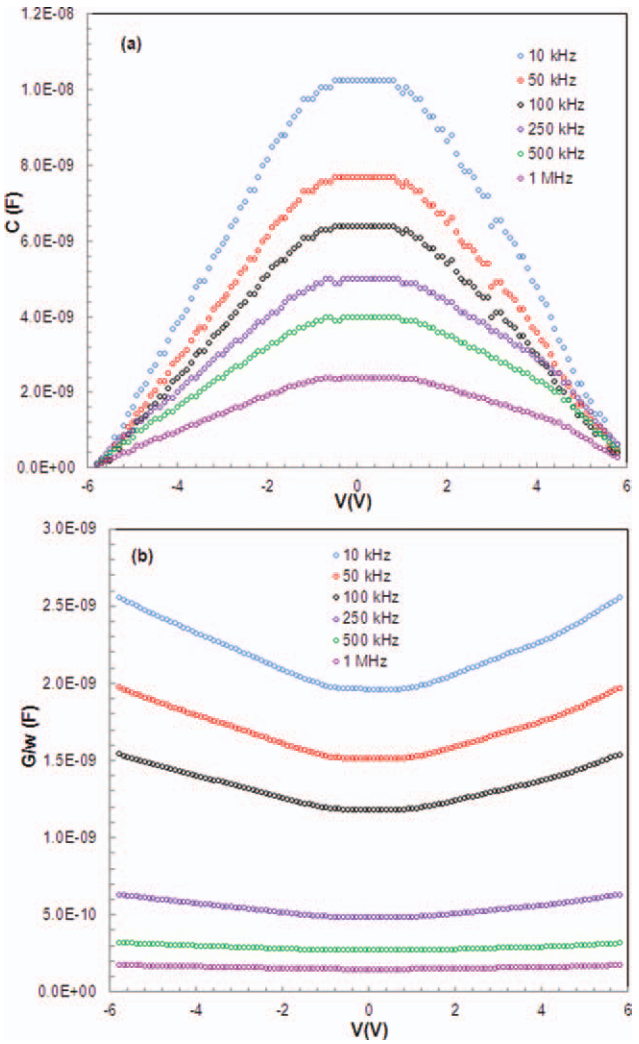

Figure 5. The voltage dependent plot of *C–V* and *G/w* for organic devices in the frequency range of 10 kHz to 1 MHz. [Color figure can be viewed in the online issue, which is available at wileyonlinelibrary.com.]

The real series resistance of MIS devices can be subtracted from the measured capacitance (C_{ma}) and conductance (G_{ma}) in strong accumulation region at high frequency.[27] In addition, voltage and frequency dependence of series resistance can be determined using *C–V* and *G/w-V* measurements. At a given frequency, to determine R_s, the MIS devices are biased into strong accumulation. Then the admittance Y_{ma} is given by[27],

$$Y_{ma} = G_{ma} + j\omega C_{ma} \tag{8}$$

R_s was calculated from the admittance measured in strong accumulation according to[27]

$$R_s = \frac{G_{ma}}{G_{ma}^2 + (\omega C_{ma})^2} \tag{9}$$

where C_{ma} and G_{ma} represent the measured capacitance and conductance in strong accumulation region.

As shown in Table I, the R_s decreases systematically with increasing frequency for each forward bias voltage. In addition, R_s values are about equal in the voltage range 0–1 V. At 1 MHz, R_s value is in good agreement with Norde and Cheung's R_s value. When the measurements are carried out at a sufficiently high frequency (>700 kHz), the charge at the interface states cannot follow AC signal. As seen in Table I, at low frequency, R_s has a high value where the interface states are intensive.

Dielectric Properties

The frequency dependence of ε',ε,$''$ and σ_{ac} were evaluated from the capacitance and conductance measurements for ITO/PEDOT : PSS/copolymer/Au device in the frequency range of 10–500 kHz. The complex permittivity can be written as[30–32]

$$\varepsilon^* = \varepsilon' - i\varepsilon'' \tag{10}$$

where ε' and ε'' are the real and the imaginary of complex permittivity, and i is the imaginary root of -1. The complex permittivity formalism has been used to describe the electrical and dielectric properties. In the ε^* formalism, in the case of admittance Y^* measurements, the following relation holds

$$\varepsilon^* = \frac{Y^*}{j\omega C_0} = \frac{C}{C_0} - i\frac{G}{\omega C_0 i} \tag{11}$$

where C and G are the measured capacitance and conductance of the dielectric material at M/S interface, and ω is the angular frequency ($\omega = 2\pi f$) of the applied electric field.[32] At the various frequencies, the real part of the complex permittivity, the dielectric constant (ε'), is calculated using the measured capacitance values at the strong accumulation region from the relation,[32]

$$\varepsilon' = \frac{C}{C_0} = \frac{Cd_i}{\varepsilon_0 A} \tag{12}$$

where C_0 is capacitance of an empty capacitor, A is the rectifier contact area of the structure in cm^{-2}, d_i is the interfacial

Table I. The $R_s(\Omega)$ Values of Organic Device in the Frequency Range of 10 kHz to1 MHz

Frequency (kHz)	0 V	0.2 V	0.4 V	0.6 V	0.8 V	1.0 V
10	287.644	287.529	287.529	287.644	288.212	307.486
50	78.702	78.671	78.671	78.70242	78.857	84.118
100	44.471	44.453	44.453	44.471	44.559	47.548
250	12.242	12.237	12.237	12.242	12.268	12.947
500	5.378	5.374	5.376	5.374	5.378	5.667
1000	4.111	4.108	4.110	4.108	4.111	4.332

insulator layer thickness, and ε_0 is the permittivity of free space charge ($\varepsilon_0 = 8.85 \times 10^{-14}$ F/cm). In the strong accumulation region, the maximum capacitance of the structure corresponds to the insulator capacitance ($C_{ac} = C_i = \varepsilon' \varepsilon_0 A/d_i$). At various frequencies, the imaginary part of the complex permittivity, the dielectric loss (ε'') are calculated using the measured conductance values from the relation,

$$\varepsilon'' = \frac{G}{\omega C_i} = \frac{G d_i}{\varepsilon_0 \omega A} \tag{13}$$

The σ_{ac} of the dielectric material can be given by the following equation,[30–32]

$$\sigma_{ac} = \omega C \tan\delta (d/A) = \varepsilon'' \omega \varepsilon_0 \tag{14}$$

Figure 6(a,b) show the voltage dependence of the real part of ε' and ε'' of ITO/PEDOT : PSS/copolymer/Au device in the frequency range of 10 kHz to 1 MHz. The values of the ε' and ε''

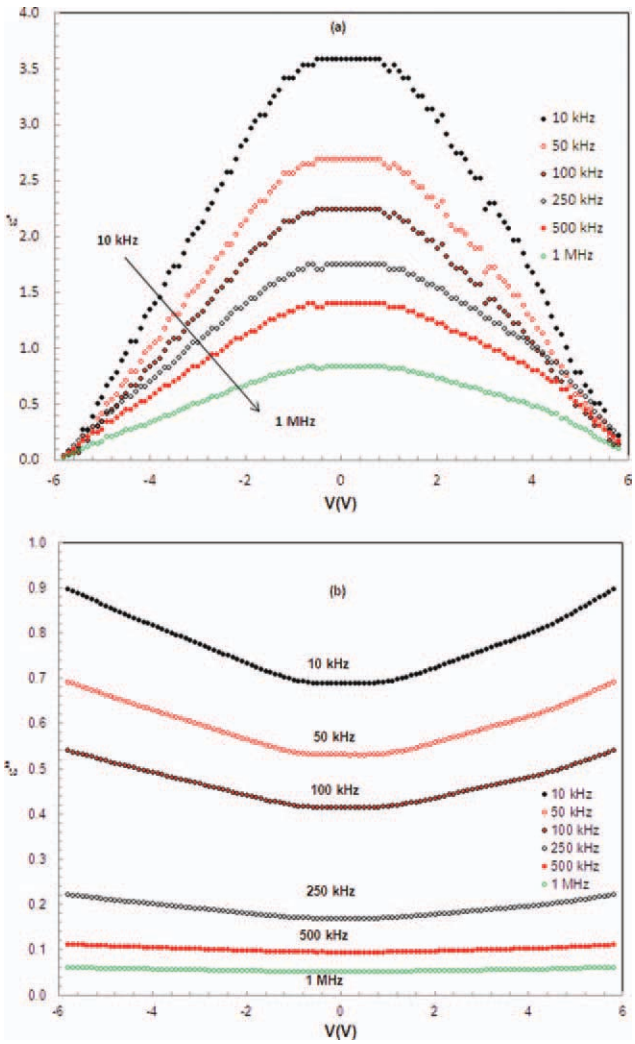

Figure 6. Voltage dependence of the (a) ε' and (b) ε'' in the frequency range of 10 kHz to1 MHz for organic device. [Color figure can be viewed in the online issue, which is available at wileyonlinelibrary.com.]

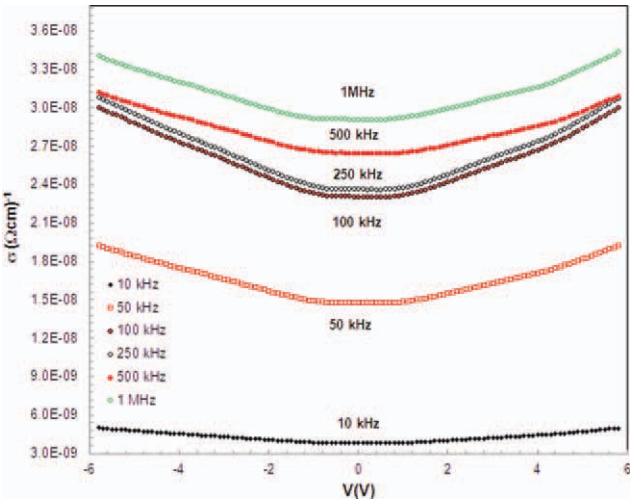

Figure 7. Voltage dependence of σ_{ac} in the frequency range of 10 kHz to 1 MHz for organic device. [Color figure can be viewed in the online issue, which is available at wileyonlinelibrary.com.]

were found strongly voltage and frequency dependent. As seen from Figure 6(a), the voltage dependence of ε' has a peak for each frequency and that of ε'' reveals a U-shaped behavior as given in Figure 6(b). The peak behavior of the ε' depends on a number of parameters; such as doping level, interface state density, series resistance of device.[14,32] It is noticed that the values of ε' increase with decreasing frequency. The reason for this may be that the polarization decreases with increasing frequency and then reaches a constant value. This may be due to the fact that beyond a certain frequency of external field, the electron hopping cannot follow the alternative field. The dispersion in ε' with frequency can be attributed to Maxwell-Wagner type interfacial polarization, that is. the fact that inhomogeneity gives rise to a frequency dependence of the conductivity as charge carries accumulate at the boundaries of less conducting regions, thereby creating interfacial polarization.[30–32] The σ_{ac} behavior of ITO/PEDOT : PSS/copolymer/Au device in the frequency range of 10 kHz to 1 MHz is presented in Figure 7. It is noticed that DC conductivity is generally increased with increasing the frequency. This DC conductivity contributes only to the dielectric loss which becomes infinite at zero frequency.[31]

CONCLUSIONS

The *I–V*, *C–V*, and *G/w–V* characteristics of benzotriazole- and fluorene-based organic devices were measured at room temperature. Electrical and dielectric properties of thin film sandwich devices have been investigated using current–voltage and capacitance–voltage methods. The φ_{Bo}, n obtained from the forward bias Ln*I-V* characteristics were found as 0.453 eV, 2.08, respectively. In addition, φ_B and n obtained from the Cheung's function and found as 0.523 eV, 2.195, respectively. The R_s values were found as 2.20, 2.12, 1.90 Ω using *dV/dLnI* versus *I*, *H(I)* versus *I*, and *F(V)-V* plots, respectively. The minimum of the *C* values coincides with the maximum of the conductance and *C* and *G/w* decrease with increasing frequency. This observation may be attributed to capacitive response of interface

states. The ε' and ε'' decrease with increasing frequency. Also, the σ_{ac} increase with increasing frequency due to the accumulation of charge carries at the boundaries. As a result, the behavior of electrical and dielectric properties especially depends on frequency, copolymer morphology, the density of space charges, and fixed surface charge for an organic device.

REFERENCES

1. Aydın, M. E.; Türüt, A. *Microelectron. Eng.* **2007,** *84*, 2875.
2. Saxena, V.; Malhotra, B. D. *Curr. Appl. Phys.* **2003,** *3*, 293.
3. Jeon, S. O.; Yook, K. S.; Lee, J. Y. *Org. Electron.* **2009,** *10*, 1583.
4. Yakuphanoglu, F.; Kandaz, M.; Senkal, B. F. *Thin Solid Films* **2008,** *516*, 8793.
5. Li, W.; Qin, R.; Andersson, M.; Li, F.; Zhang, C.; Li, B.; Liu, Z.; Bo, Z.; Zhang, F. *Polymer* **2010,** *51*, 3031.
6. Zhang, L.; He, C.; Chen, J.; Yuan, P.; Huang, L.; Zhang, C.; Cai, W.; Liu, Z.; Cao, Y. *Macromolecules* **2010,** *43*, 9771.
7. Friedel, B.; McNeill, C. R.; Greenham, N. C. *Chem. Mater.* **2010,** *22*, 3389.
8. Kroon, R.; Lenes, M.; Hummelen, J. C.; Blom, P. W. M.; Boer, B. *Polym. Rev.* **2008,** *48*, 531.
9. Balan, A.; Baran, D.; Sariciftci, N. S.; Toppare, L. *Sol. Energy Mater. Sol. Cells* **2010,** *94*, 1797.
10. Liu, B.; Ye, S.; Zou, Y.; Peng, B.; He, Y.; Zhou, K. *Macromol. Chem. Phys.* **2011,** *212*, 1489.
11. Yıldız, D. E.; Altındal, Ş.; Kanbur, H. *J. Appl. Phys.* **2008,** *103*, 124502.
12. Özer, M.; Yıldız, D. E.; Altındal, Ş.; Bülbül, M. M. *Solid-State Electron.* **2007,** *51*, 941.
13. Okur, S.; Yakuphanoglu, F.; Ozsoz, M.; Kadayifcilar, P. K. *Microelectron. Eng.* **2009,** *86*, 2305.
14. Yıldız, D. E.; Dökme, I. *J. Appl. Phys.* **2011,** *110*, 014507.
15. Pakma, O.; Serin, N.; Serin, T.; Altındal, Ş. *J. Phys. D: Appl. Phys.* **2008,** *41*, 215103.
16. Tataroglu, A.; Yücedag, İ.; Altındal, Ş. *Microelectron. Eng.* **2008,** *85*, 1518.
17. Kaya, E.; Apaydın, D. H.; Yıldız, D. E.; Toppare, L.; Cirpan, A. *Sol.Energy Mater. Sol. Cells* **2012,** *99*, 321.
18. Hill, W. A.; Coleman, C. C. *Solid-State Electron.* **1980,** *23*, 987.
19. Sze, S. M. Physics Semiconductor Devices, 2nd ed.; John Wiley & Sons Inc., New York, **1981.**
20. Rhoderick, E. H.; Williams, R. H. Metal-Semiconductor Contacts, 2nd ed.; Clarendon Press: Oxford, **1988.**
21. Abthagir, P. S.; Saraswathi, R. *Org. Electron.* **2004,** *5*, 299.
22. Ocak, Y. S.; Kulakci, M.; Turan, R.; Akkılıç, K. *Synth. Met.* **2009,** *159*, 1603.
23. Gutman, F.; Lyons, L. E. Organic Semiconductors; Gutman, F., Lyons, L. E., Eds.; Krieger Publishing Company: Malabar, FL, **1980.**
24. Cheung, S. K.; Cheung, N. W. *Appl. Phys. Lett.* **1986,** *49*, 85.
25. Norde, H. *J. Appl. Phys.* **1979,** *50*, 5052.
26. Sato, K.; Yasamura, Y. *J. Appl. Phys.* **1985,** *58*, 3656.
27. Nicollian, E. H.; Brews, J. R. MOS Physics and Techonology; Wiley: New York, **1982.**
28. Depas, M.; Van Meirhaegh, R. L.; Laflere, W. H.; Cardon, F. *Solid-State Electron.* **1994,** *37*, 433.
29. Konofaos, N.; McClean, I. P.; Thomas, C. B. *Phisica Status Solidi A* **1997,** *161*, 111.
30. Daniel, V. V. Dielectric Relaxation; Academic Press: London, **1967.**
31. Popescu, M.; Bunget, I. Physics of Solid Dielectrics; Elsevier: Amsterdam, **1984.**
32. Symth, C. P. Dielectric Behaviour and Structure; McGraw-Hill: New York, **1955.**